

Figure 1: (A) An illustration of local subgraphs distributed across multiple participants with overlapping nodes, missing edges and community structures between subgraphs. (B) Existing subgraph FL [42, 43, 46] expands the local subgraphs to tackle the missing edge problem, but collapse incompatible knowledge from heterogeneous subgraphs. (C) Our personalized subgraph FL focuses on joint improvement of local models working on interrelated subgraphs, such as ones within the same community, by selectively sharing knowledge across them. (Right:) Results on knowledge collapse, where local models belonging to two small communities (Comm 1 and 2) suffer from large performance degeneration by existing subgraph FL (e.g., FedGNN [42, 43] and FedSage [46]). A personalized FL method, FedPer [2] also underperforms ours since it only focuses on individual model’s improvement without sharing local personalization layers between similar subgraphs.

particular, in such an FL framework, each client will individually train a local GNN on the private local data, while a central server aggregates the locally updated GNN weights from multiple clients into one, and then transmits it back to the clients. Recent subgraph FL methods work in such a manner [42, 43, 46] while additionally tackling the problem of missing edges between subgraphs. This is done as illustrated in Figure 1 (B), where the local subgraph is expanded either by exactly augmenting the relevant nodes from the other subgraphs at the other clients [42, 43], or by estimating the nodes using the node information in the other subgraphs [46]. However, such sharing of node information may compromise data privacy and can incur high communication costs.

Also, there exists an even more serious issue that has been overlooked by the existing subgraph FL methods. We observe that they suffer from large performance degeneration (See Figure 1 right), due to a lack of consideration of the *heterogeneity* among the subgraphs, which is natural since subgraphs comprise different parts of a global graph. Notably, there could be multiple communities within a global graph, each of which is formed by a group of densely connected subgraphs with similar characteristics (Figure 1 (A)). For example, some of patient networks from hospitals can be grouped by their specialized sectors according to the disease categories, namely psychiatric or ophthalmology.

Motivated by this challenge, we introduce a novel problem of personalized subgraph FL, whose goal is the joint improvement of interrelated local models trained on the interconnected local subgraphs, for instance, subgraphs belonging to the same community (See Figure 1 (C)), by sharing weights among them. However, tackling personalized subgraph FL is challenging, since we do not know which subgraph each client has, due to their local accessibility. To resolve this issue, we use functional embeddings of GNNs on random graphs to obtain similarity scores between two local GNNs, and then use them to perform weighted averaging of the model weights at the server. However, the similarity scores only tell how relevant each local model from the other clients is, but not which of the parameters are relevant. Thus we further learn and apply personalized sparse masks on the local GNN at each client to obtain only the subnetwork, relevant for the local subgraph. We refer to this subgraph FL framework as *FEDerated Personalized SUBgraph learning* (FED-PUB).

We extensively validate our FED-PUB on six different datasets with varying numbers of clients, under both overlapping and disjoint subgraph FL scenarios. The experimental results show that ours significantly outperforms relevant baselines. Further analysis shows that our method can discover community structures among subgraphs, and the subgraph-specific masking localizes the knowledge with respect to subgraphs belonging to each community. Our main contributions are as follows:

- We introduce a novel problem of personalized subgraph FL, which aims at collaborative improvements of the related local models (e.g. subgraphs belonging to the same community), which has been relatively overlooked by previous works on graph and subgraph FL.
- We propose a novel framework for personalized subgraph FL, which performs weighted averaging of the local model parameters based on their functional similarities obtained without accessing the data, and learns sparse masks to select only the relevant subnetworks for the given subgraphs.
- We validate our personalized subgraph FL framework on six real-world datasets under two different settings, demonstrating its effectiveness over existing subgraph FL baselines.

## 2 Related Work

**Graph Neural Networks** Graph representation learning with Graph Neural Networks (GNNs) [11, 49, 44, 19, 3], which aims to learn the representations of the nodes, the edges, and the entire graph, is an extensively studied topic. Most existing GNNs are formulated under the message passing scheme [9] that iteratively represents a node by aggregating features from its neighboring nodes as well as itself. For example, Graph Convolutional Network (GCN) [23] approximates the spectral graph convolutions [13], yielding a mean aggregation over neighboring nodes. Similarly, for each node, GraphSAGE [12] aggregates the features from its neighbors to update the node representation. Graph Attention Network (GAT) [40] leverages the attention mechanism [4] to allocate more weights on the most relevant neighbors during aggregation. Such advances in GNNs have led to large successes on node and link prediction tasks [23, 48]. However, they are not directly applicable to the real-world systems with locally distributed graphs, where graphs from different sources are not shared across participants, which gives rise to federated learning approaches to train GNNs.

**Federated Learning** Federated Learning (FL) [31, 26, 41, 20, 25], whose objective is to learn a model by aggregating model weights trained on local data, is an essential approach for our distributed subgraph learning problem. To mention a few, FedAvg [31] locally trains a model for each client and then transmits the trained model to a server, while the server aggregates the model weights from local clients and then sends the aggregated model back to them. However, since the locally collected data from different clients may largely vary, heterogeneity is a crucial issue. To tackle this, FedProx [26] proposes the regularization term that minimizes the weight differences between local and global models, which prevents the model from diverging by overfitting to the local training data. However, when the local data is extremely heterogeneous, it is more appropriate to collaboratively train a personalized model for each client rather than learning a single global model [2, 29, 27, 47, 6]. FedPer [2] is such a personalized FL method, which shares only the base layers while having local personalized layers for each client, to keep the local knowledge. Unlike the commonly studied image and text data, graph-structured data is defined by connections between instances, and consequently introduces additional challenges: missing edges and shared nodes between private subgraphs.

**Graph Federated Learning** Few recent studies propose to use the FL framework to collaboratively train GNNs without sharing graph data [14], which can be broadly classified into subgraph- and graph-level methods. Graph-level FL methods assume that different clients have completely disjoint graphs (e.g., molecular graphs), and recent works [45, 15] focus on the heterogeneity among non-IID graphs (i.e., difference in graph labels across various clients). In contrast to graph-level FL methods that have similar challenges to general FL scenarios, the subgraph-level FL problem we target has a unique graph-structural challenge, that there exist missing yet probable links between subgraphs, since a subgraph is a part of a larger global graph. To deal with such a missing link problem among subgraphs, existing methods [42, 43, 46] augment the nodes by requesting the node information in the other subgraphs, and then connecting the existing nodes with the augmented ones. However, this scheme could compromise data privacy constraints, and also increases communication overhead across clients. Unlike existing subgraph FL that focuses on the problem of missing links, our subgraph FL method tackles the problem with a completely different perspective, focusing on discovering subgraph communities [35, 10, 34], which are groups of densely connected subgraphs.

## 3 Personalized Subgraph Federated Learning

We provide the general descriptions of Graph Neural Networks (GNNs) and Federated Learning (FL), and then define our novel problem of personalized subgraph FL lying at the intersection of them.

**Graph Neural Networks** A graph  $\mathcal{G} = (\mathcal{V}, \mathcal{E})$  consists of a set of nodes  $\mathcal{V}$  with  $n$  elements and a set of edges  $\mathcal{E}$  with  $m$  elements along with its node feature matrix  $\mathbf{X} \in \mathbb{R}^{n \times d}$ , where each column represents a  $d$ -dimensional feature for each node. Further,  $(u, v) \in \mathcal{E}$  represents an edge from a node  $u$  to a node  $v$ . Then, given the graph, Graph Neural Networks (GNNs) [9, 11] generally represent each node based on features from its neighbors as well as itself, formally defined as follows:

$$\mathbf{H}_v^{(l+1)} = \text{UPDATE}^{(l)} \left( \mathbf{H}_v^{(l)}, \text{AGGREGATE}^{(l)} \left( \left\{ \mathbf{H}_u^{(l)} : \forall u \in \mathcal{N}(v) \right\} \right) \right), \quad (1)$$

where  $\mathbf{H}_v^{(l)}$  is the feature matrix for node  $v$  at  $l$ -th layer,  $\mathcal{N}(v)$  denotes a set of adjacent nodes of node  $v$ :  $\mathcal{N}(v) = \{u \in \mathcal{V} \mid (u, v) \in \mathcal{E}\}$ , AGGREGATE aggregates the features of  $v$ 's neighbors, and UPDATE updates the node  $v$ 's representation given its previous representation and the aggregated representations from the neighbors.  $\mathbf{H}^{(1)}$  is initialized as input node features  $\mathbf{X}$ .

**Federated Learning** The objective of Federated Learning (FL) is to collaboratively train a model with local private data. Let assume that we have  $K$  participants with locally collected data that is not accessible from others:  $\mathcal{D}_k = \{\mathbf{X}_i, \mathbf{y}_i\}_{i=1}^{N_k}$ , where  $\mathbf{X}_i$  is a data instance,  $\mathbf{y}_i$  is its corresponding class label, and  $N_k$  is the number of data instances at  $k$ -th client. Then, for decentralized training with local data, a popular FL algorithm, FedAvg [31], works as the following three steps:

1. **(Initialization)** At the initial communication round  $r = 0$ , the central server first selects  $K$  clients that are available for training, and initializes their local model parameters as the global parameter  $\bar{\theta}$ , represented as follows:  $\theta_k^{(0)} \leftarrow \bar{\theta}^{(0)} \forall k$ , where  $\theta_k^{(0)}$  is the parameters for  $k$ -th client.
2. **(Local Updates)** Each active local model performs training on private local data  $\mathcal{D}_k$  to minimize the task loss  $\mathcal{L}(\mathcal{D}_k; \theta_k^{(0)})$ , consequently updating the parameters  $\theta_k^{(1)} \leftarrow \theta_k^{(0)} - \eta \nabla \mathcal{L}$ .
3. **(Global Aggregation)** After local training, the server aggregates the locally learned knowledge with respect to the number of training instances, i.e.,  $\bar{\theta}^{(1)} \leftarrow \frac{N_k}{N} \sum_{k=1}^K \theta_k^{(1)}$  with  $N = \sum_k N_k$ , and distributes the updated global parameters  $\bar{\theta}^{(1)}$  to the local clients selected at the next round.

This FL algorithm iterates between Step 2 and 3 until reaching the final round  $R$ .

**Challenges in Subgraph FL** While the above FL works well on image and text data, due to the unique structure of graphs, there exist nontrivial challenges for applying this FL scheme to graph-structured data. In particular, unlike with an image domain where each instance  $\mathbf{X}_i$  is independent from the other images, each node  $v$  in a graph is always influenced by its relationships to adjacent nodes  $\mathcal{N}(v)$ . Moreover, a local graph  $G_i$  could be a subgraph of a larger global graph  $\mathcal{G}$ :  $G_i \subseteq \mathcal{G}$ . In such a case, there could be missing edges between local subgraphs in two different clients:  $(u, v)$  with  $u \in \mathcal{V}_i$  and  $v \in \mathcal{V}_j$  for clients  $i$  and  $j$ , respectively. To tackle this missing edge problem, few existing subgraph FL methods [42, 46] estimate the nodes from a local subgraph  $G_k$  based on the node information from the subgraphs at other clients  $G_i \forall i \neq k$ , and then extend the existing nodes with the estimated ones. However, this augmentation scheme incurs high communication costs as it requires sharing node information across clients, which may also violate data privacy constraints [1].

Yet, there exists another issue that makes subgraph FL even more challenging. Assume that we have a global graph consisting of all the subgraphs. Then, there exists *communities* of such subgraphs [35, 10, 34], where subgraphs within the same community are more densely connected to each other than subgraphs outside the community. Formally, a global graph  $\mathcal{G}$  can be decomposed into  $T$  different communities:  $C_i \subseteq \mathcal{G} \forall i = 1, \dots, T$ , where  $i$ -th community  $C_i = (\mathcal{V}_i, \mathcal{E}_i)$  consists of densely connected nodes. Then, in a subgraph FL problem, each client has a local subgraph  $G_j$  that belongs to at least a single community<sup>2</sup>:  $C_i = \bigcup_{j=1}^J G_j$ . Note that, based on the theory of network homophily [32], such connected subgraphs within the same community have similar properties, while subgraphs in two opposite communities are not. Such distributional heterogeneity across communities may lead a naive FL algorithm to collapse incompatible knowledge across different communities.

**Personalized Subgraph FL** To prevent the above knowledge collapse issue, we aim to personalize the subgraph FL algorithm by performing weighted averaging of the local model parameters at the server, rather than learning a single set of global parameters; thereby capturing the subgraph community structures among interrelated subgraphs. Formally, the objective of existing subgraph FL [42, 43, 46, 28] is as follows:  $\min \sum_{G_i \subseteq \mathcal{G}} \mathcal{L}(G_i; \theta_i)$ . However, a major drawback of such a scheme is that, since subgraphs in two different communities with sparse connections are extremely heterogeneous due to network homophily [32], finding a universal set of parameters (i.e.,  $\theta$ ) that work on all tasks will result in finding a suboptimal parameter set. To address such limitations of existing subgraph FL, we formulate a novel problem of personalized subgraph FL, formalized as follows:

$$\min \sum_{G_i \subseteq \mathcal{G}} \mathcal{L}(G_i; \theta_i), \theta_i \leftarrow \sum_{j=1}^J \alpha_{ij} \theta_j \text{ with } \alpha_{ik} \gg \alpha_{il} \text{ for } G_k \subseteq C \text{ and } G_l \not\subseteq C, \quad (2)$$

where  $\theta_i$  is the weight for subgraph  $G_i$  belonging to community  $C$ , and  $\alpha_{ij}$  is the coefficient for weight aggregation which we will specify in Section 4.1. This formulation promotes the collaborative learning across multiple local models that work on the interrelated subgraphs that belong to the same community, by assigning larger weights on them.

<sup>2</sup>For simplicity, we assume that a subgraph belongs to only a single community, however, the formulation does not change even when a subgraph can belong to multiple communities.

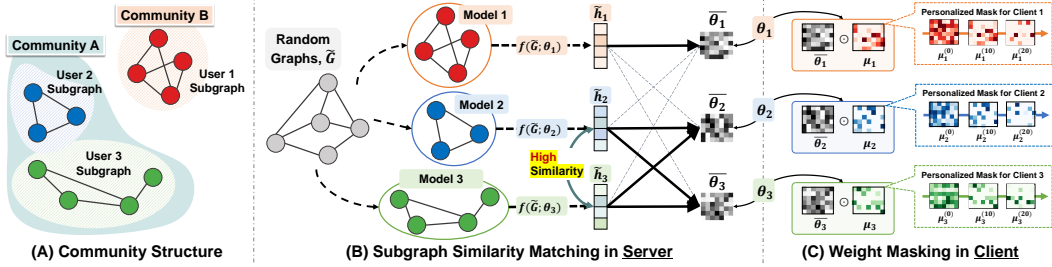


Figure 2: (A) **Two communities**, each of which consists of one/two subgraphs. (B) **Client Similarity Matching**: we forward randomly generated graphs to models  $f(\tilde{G}; \theta_i)$ , and then obtain the functional embeddings of them  $\tilde{h}_i$ , which are then used to estimate the similarities between subgraphs. The similarities are used in the weight aggregation, resulting in the personalized model weights  $\tilde{\theta}$ . (C) **Weight Masking**: the transmitted weights from the server to clients  $\tilde{\theta}$  are masked and shifted by local masks for localization to the local subgraph distribution.

## 4 Federated Personalized Subgraph Learning (FED-PUB) Framework

Our goal of personalized subgraph FL is to jointly improve the local models trained on the inter-connected local subgraphs forming the community structures. To this end, we propose to compute subgraph similarity scores for detecting communities, and to mask subgraph-irrelevant weights.

### 4.1 Subgraph Similarity Estimation for Detecting Subgraph Community

We aim to reflect the community structure consisting of a group of densely connected subgraphs, by sharing more weights among subgraphs in the same community, as formalized in equation 2. Due to network homophily where similar instances in the graph are more associated with each other [32], the subgraphs within the same community should have similar properties. Therefore, if one can measure the subgraph similarities, we can group the similar ones into the community. However, measuring the similarity between local subgraphs is a seemingly impossible goal since we do not know which subgraph each client has due to local accessibility. How can we then compute subgraph similarities, without accessing them? To this end, we aim to approximate the subgraph similarity at local clients using auxiliary information obtained from the local GNN models that work on the subgraphs.

**Subgraph Similarity Estimation with Model Parameters** For measuring the similarity between subgraphs at each client, without accessing them, we may use the model parameters as proxies, as follows:  $S(i, j) = (\theta_i \cdot \theta_j) / (\|\theta_i\| \|\theta_j\|)$ , where  $\theta$  is a flattened parameter into the vector, and  $S$  is a similarity measure. This may sound reasonable since the GNN model trained on the subgraph will embed its knowledge into its parameters. However, this scheme has a crucial drawback that similarity measured in the high-dimensional parameter space is not meaningful due to the curse of dimensionality [5], and that the cost of calculating the similarity between parameters grows rapidly as the model size increases (See Figure 3).

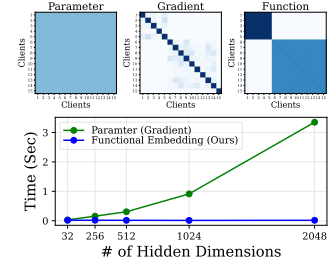


Figure 3: Effectiveness (top) and efficiencies (bottom) of different similarity measurements.

**Subgraph Similarity Estimation with Functional Embedding** To tackle the limitations of using parameter distance, we propose to measure the functional similarity of neural networks by feeding the same input to every local client and then calculating the similarities using their outputs, inspired by a work for neural network search [18]. The main intuition is that we can consider the transformation defined with a neural network as a function, and we measure the functional similarity of two networks by the distance of their outputs for the same input. However, unlike the previous work [18] that tackles image classification, which uses Gaussian noises as inputs, we use random graphs as inputs as we work with GNNs. Formally, let  $\tilde{G} = (\tilde{\mathcal{V}}, \tilde{\mathcal{E}})$  be a random community graph obtained from a stochastic block model [16], where subgraphs within the community have more edges between them than edges across the communities. Further,  $\tilde{\mathcal{V}}$  is randomly initialized from the normal distribution. Then, the similarity between two functions defined by GNNs at clients  $i$  and  $j$  is defined as follows:

$$S(i, j) = \frac{\tilde{h}_i \cdot \tilde{h}_j}{\|\tilde{h}_i\| \|\tilde{h}_j\|}, \quad \tilde{h}_i = \text{AVG}(f(\tilde{G}; \theta_i)) \text{ and } \tilde{h}_j = \text{AVG}(f(\tilde{G}; \theta_j)), \quad (3)$$

where  $\tilde{h}$  is the averaged output of all node embeddings for input  $\tilde{G}$  with AVG operation to reduce the dimensionality of the output from  $n \times d$  to  $d$ , for  $n$  nodes with  $d$ -dimensional node features.

**Personalized Weight Aggregation based on Subgraph Similarity** With equation 3, the remaining step is then to share the model weights between models working on similar subgraphs belonging to the same community. However, entirely ignoring the model parameters from different communities may result in exploiting only the local objective while ignoring globally useful weights, which may result in performance degeneration. Therefore, we perform weighted averaging of all the local models from the other clients based on their functional (subgraph) similarities, as follows (Figure 2 (B)):

$$\bar{\theta}_i \leftarrow \sum_j \alpha_{ij} \cdot \theta_j, \quad \alpha_{ij} = \frac{\exp(\tau \cdot S(i, j))}{\sum_k \exp(\tau \cdot S(i, k))}, \quad (4)$$

where  $\alpha_{ij}$  is a normalized similarity between clients  $i$  and  $j$ , and  $\tau$  is a hyperparameter for scaling the unnormalized similarity score. Note that increasing the value of  $\tau$  (e.g., 10) will result in model averaging done almost exclusively among subgraphs detected as belonging to the same community.

This personalized scheme handles two challenges in subgraph FL. First, in contrast to the global weight aggregation scheme which easily collapses the knowledge from heterogeneous communities into a single model, our subgraph FL allows the models belonging to different communities to obtain model weights that are beneficial for each community. Also, the missing edges between subgraphs that have been explicitly handled by previous works [42, 43, 46] could be also implicitly considered by assigning larger weights to models within the same community (See Figure 10). This also enhances data privacy while minimizing the communication costs between probably linked subgraphs.

#### 4.2 Adaptive Weight Masking for Selecting Subgraph-Relevant Parameters

With the previous similarity matching scheme, we can effectively group GNN models that belong to the same community, thus preventing the collapsing of irrelevant knowledge from other communities. However, the scalar weighting scheme only considers how much each local model from other clients is relevant for the subgraph task, but not *which* parameters are relevant. Thus we propose a scheme to select only the relevant parameters from the aggregated model weights transmitted from the server.

**Personalized Parameter Masking** We perform selective training and updating of the aggregated parameters by modulating and shifting them, using sparse local masks. Let  $\mu_k$  be a local mask for a client  $k$ . Then, our local model weight is obtained by modulating the weights from the server, as follows:  $\theta_k = \bar{\theta}_k \odot \mu_k$ , where  $\odot$  is an element-wise multiplication operation between the globally given weight  $\bar{\theta}_k$  and the local mask  $\mu_k$ . Note that the local mask is a free variable and is not shared across clients. Also, we initialize  $\mu_k$  as ones, in order to start training with the globally initialized model parameters. We then further promote sparsity on the mask, which brings two key advantages. First, we can transmit only the partial parameters, that have not been sparsified at the client to the server rather than sending all parameters, thus reducing the communication costs. Moreover, if local masks are sufficiently sparse, the local models can be trained faster, given that zero-skipping operations are supported (Figure 2 (C)). To take these benefits, we use  $L_1$  regularizer on  $\mu_k$  when performing local optimization (See Section B.3 for details on sparsification), as shown in equation 5.

**Preventing Local Divergence with Proximal Term** As masks are trained only with limited local data without parameter sharing, they may be easily overfitted to the training instances in each client. To alleviate this issue, we adopt the proximal term proposed in Li et al. [26] that regularizes the locally updated models  $\theta_k$  to be closer to the globally given model  $\bar{\theta}_k$ , therefore, preventing the model from extremely drifting to the local training distribution. To sum up, at  $k$ -th client, our objective function including sparsity and proximal terms with  $L_1$  and  $L_2$  losses is denoted as follows:

$$\min_{(\theta_k, \mu_k)} \mathcal{L}(\mathcal{D}_k; \theta_k, \mu_k) + \lambda_1 \|\mu_k\|_1 + \lambda_2 \|\theta_k - \bar{\theta}_k\|_2^2, \quad (5)$$

where  $\mathcal{L}$  is the conventional cross-entropy loss function, and  $\lambda_1$  and  $\lambda_2$  are scaling hyper-parameters.

## 5 Experiments

We now experimentally validate our FED-PUB on six different datasets under both the overlapping and disjoint subgraph scenarios with varying client numbers, with node classification tasks.

### 5.1 Experimental Setups

**Datasets** Following the experimental setup from Zhang et al. [46], we construct the distributed subgraphs from the benchmark dataset by dividing it into the number of participants, each of which has a subgraph that is a part of an original graph. Specifically, we use six datasets: Cora, CiteSeer,

Table 1: **Results on the overlapping node scenario.** The reported results are mean and standard deviation over three different runs. Only the statistically significant performances ( $p > 0.05$ ) are highlighted in bold.

Methods	Cora			CiteSeer			Pubmed			
	10 Clients	30 Clients	50 Clients	10 Clients	30 Clients	50 Clients	10 Clients	30 Clients	50 Clients	
Local	73.98 ± 0.25	71.65 ± 0.12	76.63 ± 0.10	65.12 ± 0.08	64.54 ± 0.42	66.68 ± 0.44	82.32 ± 0.07	80.72 ± 0.16	80.54 ± 0.11	-
FedAvg	76.48 ± 0.36	53.99 ± 0.98	53.99 ± 4.53	69.48 ± 0.15	66.15 ± 0.64	66.51 ± 1.00	82.67 ± 0.11	82.05 ± 0.12	80.24 ± 0.35	-
FedProx	77.85 ± 0.50	51.38 ± 1.74	56.27 ± 9.04	69.39 ± 0.35	66.11 ± 0.75	66.53 ± 0.43	82.63 ± 0.17	82.13 ± 0.13	80.50 ± 0.46	-
FedPer	78.73 ± 0.31	74.18 ± 0.24	74.42 ± 0.37	69.81 ± 0.28	65.19 ± 0.81	67.64 ± 0.44	85.31 ± 0.06	84.35 ± 0.38	83.94 ± 0.10	-
GCFL	78.84 ± 0.26	73.41 ± 0.27	76.63 ± 0.16	69.48 ± 0.39	64.92 ± 0.18	65.98 ± 0.30	83.59 ± 0.25	80.77 ± 0.12	81.36 ± 0.11	-
FedGNN	70.63 ± 0.83	61.38 ± 2.33	56.91 ± 0.82	68.72 ± 0.39	59.98 ± 1.52	58.98 ± 0.98	84.25 ± 0.07	82.02 ± 0.22	81.85 ± 0.10	-
FedSage	77.52 ± 0.46	51.99 ± 0.42	55.48 ± 11.5	68.75 ± 0.48	65.97 ± 0.02	65.93 ± 0.30	82.77 ± 0.08	82.14 ± 0.11	80.31 ± 0.68	-
FED-PUB (Ours)	<b>79.60 ± 0.12</b>	<b>75.40 ± 0.54</b>	<b>77.84 ± 0.23</b>	<b>70.58 ± 0.20</b>	<b>68.33 ± 0.45</b>	<b>69.21 ± 0.30</b>	<b>85.70 ± 0.08</b>	<b>85.16 ± 0.10</b>	<b>84.84 ± 0.12</b>	-

Methods	Amazon-Computer			Amazon-Photo			ogbn-arxiv			All
	10 Clients	30 Clients	50 Clients	10 Clients	30 Clients	50 Clients	10 Clients	30 Clients	50 Clients	
Local	88.50 ± 0.20	86.66 ± 0.00	87.04 ± 0.02	92.17 ± 0.12	90.16 ± 0.12	90.42 ± 0.15	62.52 ± 0.07	61.32 ± 0.04	60.04 ± 0.24	76.72
FedAvg	88.99 ± 0.19	83.37 ± 0.47	76.34 ± 0.12	92.91 ± 0.07	89.30 ± 0.22	74.19 ± 0.57	63.56 ± 0.02	59.72 ± 0.06	60.94 ± 0.24	73.38
FedProx	88.84 ± 0.20	83.84 ± 0.89	76.60 ± 0.47	92.67 ± 0.19	89.17 ± 0.40	72.36 ± 2.06	63.52 ± 0.11	59.86 ± 0.16	61.12 ± 0.04	73.38
FedPer	89.30 ± 0.04	87.99 ± 0.23	88.22 ± 0.27	92.88 ± 0.24	91.23 ± 0.16	90.92 ± 0.38	63.97 ± 0.08	62.29 ± 0.04	61.24 ± 0.11	78.42
GCFL	89.01 ± 0.22	87.24 ± 0.09	87.02 ± 0.22	92.45 ± 0.10	90.58 ± 0.11	90.54 ± 0.08	63.24 ± 0.02	61.66 ± 0.10	60.32 ± 0.01	77.61
FedGNN	88.15 ± 0.09	87.00 ± 0.10	83.96 ± 0.88	91.47 ± 0.11	87.91 ± 1.34	78.90 ± 6.46	63.08 ± 0.19	60.09 ± 0.04	60.51 ± 0.11	73.66
FedSage	89.24 ± 0.15	81.33 ± 1.20	76.72 ± 0.39	92.76 ± 0.05	88.69 ± 0.99	72.41 ± 1.36	63.24 ± 0.02	59.90 ± 0.12	60.95 ± 0.09	73.12
FED-PUB (Ours)	<b>89.98 ± 0.12</b>	<b>89.15 ± 0.06</b>	<b>88.76 ± 0.14</b>	<b>93.22 ± 0.07</b>	<b>92.01 ± 0.07</b>	<b>91.71 ± 0.11</b>	<b>64.18 ± 0.04</b>	<b>63.34 ± 0.12</b>	<b>62.55 ± 0.12</b>	<b>79.53</b>

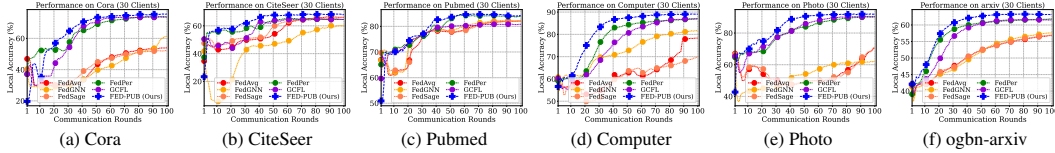


Figure 4: **Convergence plots for the overlapping node scenario.** We visualize the test accuracy curves for all six datasets corresponding to Table 1, over 100 communication rounds with 10 clients.

Pubmed and ogbn-arxiv for citation graphs [38, 17]; Amazon-Computer and -Photo for product graphs [30, 39]. We then divide the original graph into multiple subgraphs using the METIS graph partitioning algorithm [21] that can specify the number of subsets (i.e., clients for FL). For the non-overlapping scenario where there are no duplicate nodes between subgraphs, we directly use the output from the METIS as it provides the non-overlapping partitions. Meanwhile, for the overlapping scenario where nodes are duplicated between subgraphs, we randomly sample the subgraphs multiple times from the partitioned graph. For more details, please see Section B of the appendix.

**Baselines** 1) **FedAvg** [31] and 2) **FedProx** [26]: The most popular FL baselines. 3) **FedPer** [2]: A personalized FL baseline without sharing personalized layers. 4) **FedGNN (FedPerGNN)**<sup>3</sup> [42, 43] and 5) **FedSage** [46]: Subgraph FL baselines which we mainly target. 6) **GCFL** [45]: A graph FL baseline which learns completely disjoint graphs as in clustered FL [37], adopted for subgraph FL. 7) **Local**: A baseline without sharing weights with other clients. 8) **FED-PUB**: Our personalized subgraph FL including subgraph similarity matching and weight masking. See Section B for details.

**Implementation Details** We set the GCN [23] with two layers as the base GNN for all models. We perform federated learning over 100 communication rounds for Cora, CiteSeer and Pubmed datasets, while 200 rounds for the other datasets, considering the size of datasets. The local training epoch is selected in the range of {1, 2, 3} depending on the dataset size (e.g., Computer is three while CiteSeer is one)<sup>4</sup>. We then measure the node classification accuracy on subgraphs at the client-side, and then average the performance across clients. We provide further details in Section B of the appendix.

## 5.2 Experimental Results

**Main Results** Table 1 shows the node classification performance under the overlapping subgraph scenario, in which our FED-PUB statistically ( $p > 0.05$ ) significantly outperforms all the baselines. In particular, while FedGNN and FedSage are two pioneer works for the subgraph FL problem, they significantly underperform personalized FL methods including ours, especially at the larger number of clients. This is even surprising as they share node information between clients for handling the missing edge problem, yet we suppose such inferior performance comes from naive averaging of local weights without consideration of community structures. While personalized FL baselines including FedPer and GCFL show decent performance by alleviating the knowledge collapse between subgraphs with local parameters or clustering, they still largely underperform ours as they are not concerned with the aggregation between similar subgraphs that form a community (i.e., GCFL uses a bi-partitioning scheme where it iteratively divides a group of subgraphs within the same community into two disjoint sets). We then further conduct the experiments on the disjoint subgraph scenarios

<sup>3</sup>FedGNN is extended to FedPerGNN, where the core algorithm of averaging all client gradients is the same.

<sup>4</sup>We found communication rounds and local epochs are important factors to prevent overfitting of all models.

Table 2: **Results on the non-overlapping node scenario.** The reported results are mean and standard deviation over three different runs. Only the statistically significant performances ( $p > 0.05$ ) are highlighted in bold.

Methods	Cora			CiteSeer			Pubmed			-
	5 Clients	10 Clients	20 Clients	5 Clients	10 Clients	20 Clients	5 Clients	10 Clients	20 Clients	-
Local	81.30 ± 0.21	79.94 ± 0.24	80.30 ± 0.25	69.02 ± 0.05	67.82 ± 0.13	65.98 ± 0.17	84.04 ± 0.18	82.81 ± 0.39	82.65 ± 0.03	-
FedAvg	74.45 ± 5.64	69.19 ± 0.67	69.50 ± 3.58	71.06 ± 0.60	63.61 ± 3.59	64.68 ± 1.83	79.40 ± 0.11	82.71 ± 0.29	80.97 ± 0.26	-
FedProx	72.03 ± 4.56	60.18 ± 7.04	48.22 ± 6.81	71.73 ± 1.11	63.33 ± 3.25	64.85 ± 1.35	79.45 ± 0.25	82.55 ± 0.24	80.50 ± 0.25	-
FedPer	81.68 ± 0.40	79.35 ± 0.04	78.01 ± 0.32	70.41 ± 0.32	70.53 ± 0.28	66.64 ± 0.27	85.80 ± 0.21	84.20 ± 0.28	84.72 ± 0.31	-
GCFL	81.47 ± 0.65	78.66 ± 0.27	79.21 ± 0.70	70.34 ± 0.57	69.01 ± 0.12	66.33 ± 0.05	85.14 ± 0.33	84.18 ± 0.19	83.94 ± 0.36	-
FedGNN	81.51 ± 0.68	70.12 ± 0.99	70.10 ± 3.52	69.06 ± 0.92	55.52 ± 3.17	52.23 ± 6.00	79.52 ± 0.23	83.25 ± 0.45	81.61 ± 0.59	-
FedSage	72.97 ± 5.94	69.05 ± 1.59	57.97 ± 12.6	70.74 ± 0.69	65.63 ± 3.10	65.46 ± 0.74	79.57 ± 0.24	82.62 ± 0.31	80.82 ± 0.25	-
FED-PUB (Ours)	<b>83.70 ± 0.19</b>	<b>81.54 ± 0.12</b>	<b>81.75 ± 0.56</b>	<b>72.68 ± 0.44</b>	<b>72.35 ± 0.53</b>	<b>67.62 ± 0.12</b>	<b>86.79 ± 0.09</b>	<b>86.28 ± 0.18</b>	<b>85.53 ± 0.30</b>	-

Methods	Amazon-Computer			Amazon-Photo			ogbn-arxiv			All
	5 Clients	10 Clients	20 Clients	5 Clients	10 Clients	20 Clients	5 Clients	10 Clients	20 Clients	Avg.
Local	89.22 ± 0.13	88.91 ± 0.17	89.52 ± 0.20	91.67 ± 0.09	91.80 ± 0.02	90.47 ± 0.15	66.76 ± 0.07	64.92 ± 0.09	65.06 ± 0.05	79.57
FedAvg	84.88 ± 1.96	79.54 ± 0.23	74.79 ± 0.24	89.89 ± 0.83	83.15 ± 3.71	81.35 ± 1.04	65.54 ± 0.07	64.44 ± 0.10	63.24 ± 0.13	74.58
FedProx	85.25 ± 1.27	83.81 ± 1.09	73.05 ± 1.30	90.38 ± 0.48	80.92 ± 4.64	82.32 ± 0.29	65.21 ± 0.20	64.37 ± 0.18	63.03 ± 0.04	72.84
FedPer	89.67 ± 0.34	89.73 ± 0.04	87.86 ± 0.43	91.44 ± 0.37	91.76 ± 0.23	90.59 ± 0.06	66.87 ± 0.05	64.99 ± 0.18	64.66 ± 0.11	79.94
GCFL	89.07 ± 0.91	90.03 ± 0.16	89.08 ± 0.25	91.99 ± 0.29	92.06 ± 0.25	90.79 ± 0.17	66.80 ± 0.12	65.09 ± 0.08	65.08 ± 0.04	79.90
FedGNN	88.08 ± 0.15	88.18 ± 0.41	83.16 ± 0.13	90.25 ± 0.70	87.12 ± 2.01	81.00 ± 4.48	65.47 ± 0.22	64.21 ± 0.32	63.80 ± 0.05	75.23
FedSage	85.04 ± 0.61	80.50 ± 1.30	70.42 ± 0.85	90.77 ± 0.44	76.81 ± 8.24	80.58 ± 1.15	65.69 ± 0.09	64.52 ± 0.14	63.31 ± 0.20	73.47
FED-PUB (Ours)	<b>90.74 ± 0.05</b>	<b>90.55 ± 0.13</b>	<b>90.12 ± 0.09</b>	<b>93.29 ± 0.19</b>	<b>92.73 ± 0.18</b>	<b>91.92 ± 0.12</b>	<b>67.77 ± 0.09</b>	<b>66.58 ± 0.08</b>	<b>66.64 ± 0.12</b>	<b>81.59</b>

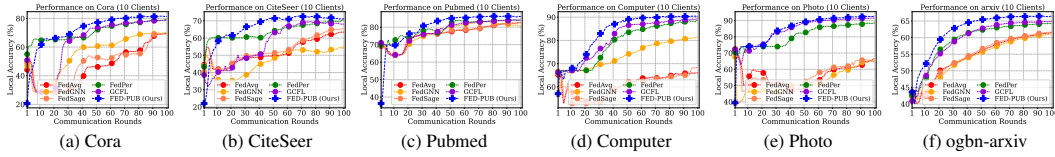


Figure 5: **Convergence plots for the non-overlapping node scenario.** We visualize the test accuracy curves for all six datasets corresponding to Table 2, over 100 communication rounds with 10 clients.

(non-overlapping scenario), where nodes are not overlapped between subgraphs, which makes the subgraph FL problem more heterogeneous. As shown in Table 2, FED-PUB consistently outperforms all existing baselines in such a challenging scenario, demonstrating the efficacy of ours.

**Fast Local Convergence** As shown in Figure 4 and 5, our FED-PUB converges rapidly, compared against baselines including personalized FL models. We conjecture that this is because, not only ours accurately identifies subgraphs forming the community and then shares weights largely across them for promoting the joint improvement of them, but also masking subgraph-irrelevant weights received from the server for localization to local subgraphs, demonstrated in the next two paragraphs.

**Accurate Community Detection** We aim to show whether FED-PUB accurately groups subgraphs comprising a community during weight aggregation. If two different subgraphs have many missing edges or have similar label distributions, we usually regard those two as within the same community [35, 10, 34]. Thereby, as shown in Figure 6 (a) and (b), there are four different communities by the interval of five, and the last two communities further comprise a larger community. Then, as shown in Figure 6 (c) and (d), FED-PUB detects obvious four communities at the first few rounds, and then captures the larger yet somewhat less-obvious community consisting of two smaller communities.

**Ablation Study** To analyze the contribution of each component, we conduct the ablation studies. As shown in Figure 7, we observe that each of our subgraph similarity matching and weight masking significantly improves the performances from the naive FedAvg, while the performance is much improved when using both together. However, the benefit from each component is different across overlapping and non-overlapping scenarios. In particular, in the former scenario where a group of highly overlapped subgraphs usually comprise a community, similarity matching for community detection is more beneficial since capturing the community would promote the joint improvement of subgraphs belonging to the same community. However, in the non-overlapping scenarios, subgraphs within the same community become lesser similar, thus selectively using the aggregated model weights from the server with personalized weight masks improves the performance a lot.

**Communication Efficiency** Another notable advantage of using the sparse masks is that we can reduce the communication costs at every FL round, as well as the model size for faster training, which we demonstrate in Table 8. In particular, Table 8 shows that existing subgraph FL methods require more than two times larger communications costs, measured by adding both the client-to-server and server-to-client costs, compared against the naive FedAvg, since they require to transfer additional node information between clients for estimating the probable nodes on the subgraphs. Contrarily, our FED-PUB has significantly lower communication costs and lower model sizes by using the sparse masks on the model weights: transmitting and training with only the partial parameters not sparsified at the client. Further, as shown in ours variants in Table 8, we can manage the trade-off between the model sparsity and the performance by controlling the hyperparameter for sparsity regularization,  $\lambda_1$ .



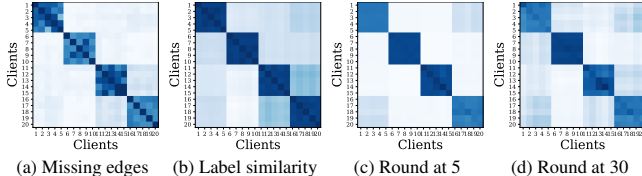


Figure 6: **The heatmaps of the community structure** on the overlapping node scenario with Cora (20 clients). Dark color indicates high similarity. (a) and (b) represent the data-level community structures, captured by our FED-PUB in (c) and (d) at round 5 and 30.

Model	Acc. [%]	Model Size [%]	Cost [%]
FedAvg	76.48 ± 0.36	100.00 ± 0.00	100.00 ± 0.00
FedGNN	70.63 ± 0.83	100.00 ± 0.00	214.94 ± 0.00
FedSage	77.52 ± 0.46	100.00 ± 0.00	276.84 ± 0.00
GCFL	78.84 ± 0.26	100.00 ± 0.00	100.00 ± 0.00
<b>Ours</b> ( $\lambda_1=9e-1$ )	77.36 ± 0.99	<b>25.13 ± 0.34</b>	<b>37.70 ± 0.56</b>
<b>Ours</b> ( $\lambda_1=7e-1$ )	79.46 ± 0.41	42.59 ± 1.33	63.89 ± 1.99
<b>Ours</b> ( $\lambda_1=5e-1$ )	<b>79.89 ± 0.12</b>	57.07 ± 0.52	85.61 ± 0.78

Figure 8: **Analysis on efficiencies** of communication costs and model sizes.

### Varying Local Epochs

As shown in Figure 9, when we increase the number of communication rounds and the local steps, the model diverges to the local subgraphs (i.e., overfitting), due to the small number of training instances and the direct connection between training and test nodes: struggle to generalize to the test instances. However, our model with the proximal term in equation 5 alleviates this issue, therefore, maintaining the highest local performance. Notably, the performance with five local epochs is inferior to the performance of one epoch, which indicates that increasing the local epochs does not always bring advantages and properly tuning them is important for subgraph FL.

### Handling Missing Edges

To measure whether FED-PUB can handle the missing edge problem: information is not shared between two neighboring subgraphs due to the missing edges, we use the local model trained on the local subgraph for evaluating the performance on its neighboring subgraph, in which the local subgraph has the most missing edges to its neighboring subgraph. Specifically, in Figure 10, (Neighbor) denotes the subgraph performance evaluated by its neighbor model, while (Local) denotes the subgraph performance from its own local model. Then, the high performance on (Neighbor) measure means two associated subgraphs share meaningful knowledge without having explicit edges between them, thereby solving the missing edge problem. Note that, existing subgraph FL explicitly augments the nodes and edges for capturing the potential information flow over the missing edges between subgraphs, while ours implicitly shares weights a lot across similar subgraphs within the same community. Figure 10 shows that ours achieves the significantly superior performance on the neighboring subgraph problem against subgraph FL baselines, which confirms that ours has an advantage on the missing edge problem by meaningfully sharing knowledge between two subgraphs having potentially missing edges, without explicitly estimating them.

## 6 Conclusion

We introduced a novel problem of personalized subgraph FL, which focuses on the joint improvement of local GNNs working on interrelated subgraphs (e.g. subgraphs belonging to the same community), by selectively utilizing knowledge from other models. The proposed personalized subgraph FL is highly challenging due to 1) difficulty of computing similarities between local subgraphs that are only locally accessible, and 2) knowledge collapse among local models that work on heterogeneous subgraphs during weight aggregation. To this end, we proposed a novel personalized subgraph FL framework, referred to as FEDerated Personalized sUBgraph learning (FED-PUB), which computes the similarities across subgraphs using functional embeddings of their local GNNs on random graphs, and uses them to perform a weighted average of the local models for each client. Further, we mask out globally given weights to focus on only the relevant subnetwork for each client (or community). We extensively validated our framework on multiple benchmark datasets with both overlapping and non-overlapping subgraphs, on which our FED-PUB significantly outperforms relevant baselines. Further analyses show the effectiveness of the subgraph similarity matching for detecting the community structures, as well as the weight masking for tackling the subgraph heterogeneity. We provide the limitations and potential societal impacts of our work in Section D of the appendix.

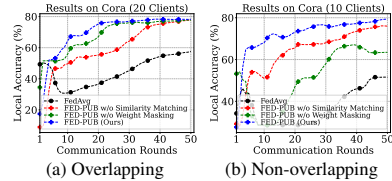


Figure 7: **Ablation studies** of our FED-PUB on both the overlapping (a) and non-overlapping (b) subgraph scenarios, on the Cora dataset.

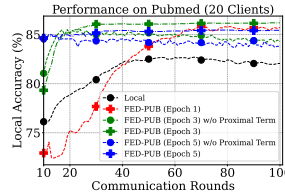


Figure 9: **Varying the local epochs** with accuracy curves.

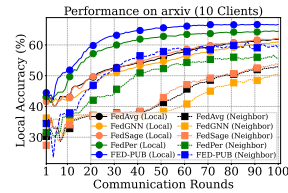


Figure 10: **Performance on neighboring subgraphs**.

## References

- [1] Martin Abadi, Andy Chu, Ian Goodfellow, H Brendan McMahan, Ilya Mironov, Kunal Talwar, and Li Zhang. Deep learning with differential privacy. In *Proceedings of the 2016 ACM SIGSAC conference on computer and communications security*, pages 308–318, 2016.
- [2] Manoj Ghuhana Arivazhagan, Vinay Aggarwal, Aaditya Kumar Singh, and Sunav Choudhary. Federated learning with personalization layers, 2019.
- [3] Jinheon Baek, Minki Kang, and Sung Ju Hwang. Accurate learning of graph representations with graph multiset pooling. In *9th International Conference on Learning Representations, ICLR 2021, Virtual Event, Austria, May 3-7, 2021*, 2021.
- [4] Dzmitry Bahdanau, Kyunghyun Cho, and Yoshua Bengio. Neural machine translation by jointly learning to align and translate. In *3rd International Conference on Learning Representations, ICLR 2015, San Diego, CA, USA, May 7-9, 2015, Conference Track Proceedings*, 2015.
- [5] Richard Bellman. Dynamic programming. *Science*, 153(3731):34–37, 1966.
- [6] Fengwen Chen, Guodong Longr, Zonghan Wu, Tianyi Zhou, and Jing Jiang. Personalized federated learning with structure. *arXiv preprint arXiv:2203.00829*, 2022.
- [7] Laxman Dhulipala, Igor Kabiljo, Brian Karrer, Giuseppe Ottaviano, Sergey Pupyrev, and Alon Shalita. Compressing graphs and indexes with recursive graph bisection. In *Proceedings of the 22nd ACM SIGKDD International Conference on Knowledge Discovery and Data Mining, San Francisco, CA, USA, August 13-17, 2016*, pages 1535–1544. ACM, 2016.
- [8] Matthias Fey and Jan E. Lenssen. Fast graph representation learning with PyTorch Geometric. In *ICLR Workshop on Representation Learning on Graphs and Manifolds*, 2019.
- [9] Justin Gilmer, Samuel S. Schoenholz, Patrick F. Riley, Oriol Vinyals, and George E. Dahl. Neural message passing for quantum chemistry. In *Proceedings of the 34th International Conference on Machine Learning, ICML 2017, Sydney, NSW, Australia, 6-11 August 2017*, volume 70 of *Proceedings of Machine Learning Research*, pages 1263–1272. PMLR, 2017.
- [10] M. Girvan and M. E. J. Newman. Community structure in social and biological networks. *Proceedings of the National Academy of Sciences*, 99(12):7821–7826, 2002.
- [11] William L. Hamilton. Graph representation learning. *Synthesis Lectures on Artificial Intelligence and Machine Learning*, 14(3):1–159.
- [12] William L. Hamilton, Zhitao Ying, and Jure Leskovec. Inductive representation learning on large graphs. In *Advances in Neural Information Processing Systems 30: Annual Conference on Neural Information Processing Systems 2017, December 4-9, 2017, Long Beach, CA, USA*, pages 1024–1034, 2017.
- [13] David K. Hammond, Pierre Vandergheynst, and Rémi Gribonval. Wavelets on graphs via spectral graph theory. *Applied and Computational Harmonic Analysis*, 30(2):129–150, 2011.
- [14] Chaoyang He, Keshav Balasubramanian, Emir Ceyani, Carl Yang, Han Xie, Lichao Sun, Lifang He, Liangwei Yang, Philip S Yu, Yu Rong, et al. Fedgraphnn: A federated learning system and benchmark for graph neural networks. *arXiv preprint arXiv:2104.07145*, 2021.
- [15] Chaoyang He, Emir Ceyani, Keshav Balasubramanian, Murali Annavaram, and Salman Avestimehr. Spreadgnn: Serverless multi-task federated learning for graph neural networks. *AAAI*, 2022.
- [16] Paul W. Holland, Kathryn Blackmond Laskey, and Samuel Leinhardt. Stochastic blockmodels: First steps. *Social Networks*, 5(2):109–137, 1983. ISSN 0378-8733.
- [17] Weihua Hu, Matthias Fey, Marinka Zitnik, Yuxiao Dong, Hongyu Ren, Bowen Liu, Michele Catasta, and Jure Leskovec. Open graph benchmark: Datasets for machine learning on graphs. *Advances in neural information processing systems*, 33:22118–22133, 2020.

- [18] Wonyong Jeong, Hayeon Lee, Geon Park, Eunyoung Hyung, Jinheon Baek, and Sung Ju Hwang. Task-adaptive neural network search with meta-contrastive learning. In *Advances in Neural Information Processing Systems*, 2021.
- [19] Jaehyeong Jo, Jinheon Baek, Seul Lee, Dongki Kim, Minki Kang, and Sung Ju Hwang. Edge representation learning with hypergraphs. In M. Ranzato, A. Beygelzimer, Y. Dauphin, P.S. Liang, and J. Wortman Vaughan, editors, *Advances in Neural Information Processing Systems*, volume 34, pages 7534–7546. Curran Associates, Inc., 2021.
- [20] Sai Praneeth Karimireddy, Satyen Kale, Mehryar Mohri, Sashank J. Reddi, Sebastian U. Stich, and Ananda Theertha Suresh. SCAFFOLD: stochastic controlled averaging for federated learning. In *Proceedings of the 37th International Conference on Machine Learning, ICML 2020, 13-18 July 2020, Virtual Event*, volume 119 of *Proceedings of Machine Learning Research*, pages 5132–5143. PMLR, 2020.
- [21] George Karypis and Vipin Kumar. Metis – unstructured graph partitioning and sparse matrix ordering system, version 2.0. Technical report, 1995.
- [22] Diederik P. Kingma and Jimmy Ba. Adam: A method for stochastic optimization. In *3rd International Conference on Learning Representations, ICLR 2015, San Diego, CA, USA, May 7-9, 2015, Conference Track Proceedings*, 2015.
- [23] Thomas N. Kipf and Max Welling. Semi-supervised classification with graph convolutional networks. In *5th International Conference on Learning Representations, ICLR 2017, Toulon, France, April 24-26, 2017, Conference Track Proceedings*, 2017.
- [24] Jure Leskovec, Lada A. Adamic, and Bernardo A. Huberman. The dynamics of viral marketing. *ACM Trans. Web*, 1(1):5, 2007.
- [25] Qinbin Li, Bingsheng He, and Dawn Song. Model-contrastive federated learning. In *IEEE Conference on Computer Vision and Pattern Recognition, CVPR 2021, virtual, June 19-25, 2021*, pages 10713–10722. Computer Vision Foundation / IEEE, 2021.
- [26] Tian Li, Anit Kumar Sahu, Manzil Zaheer, Maziar Sanjabi, Ameet Talwalkar, and Virginia Smith. Federated optimization in heterogeneous networks. In *Proceedings of Machine Learning and Systems 2020, MLSys 2020, Austin, TX, USA, March 2-4, 2020*. mlsys.org, 2020.
- [27] Paul Pu Liang, Terrance Liu, Liu Ziyin, Nicholas B. Allen, Randy P. Auerbach, David Brent, Ruslan Salakhutdinov, and Louis-Philippe Morency. Think locally, act globally: Federated learning with local and global representations, 2020.
- [28] Zhiwei Liu, Liangwei Yang, Ziwei Fan, Hao Peng, and Philip S Yu. Federated social recommendation with graph neural network. *arXiv preprint arXiv:2111.10778*, 2021.
- [29] Yishay Mansour, Mehryar Mohri, Jae Ro, and Ananda Theertha Suresh. Three approaches for personalization with applications to federated learning, 2020.
- [30] Julian McAuley, Christopher Targett, Qinfeng Shi, and Anton Van Den Hengel. Image-based recommendations on styles and substitutes. In *Proceedings of the 38th international ACM SIGIR conference on research and development in information retrieval*, pages 43–52, 2015.
- [31] H. Brendan McMahan, Eider Moore, Daniel Ramage, Seth Hampson, and Blaise Agüera y Arcas. Communication-efficient learning of deep networks from decentralized data. In *AISTATS*, 2017.
- [32] Miller McPherson, Lynn Smith-Lovin, and James M Cook. Birds of a feather: Homophily in social networks. *Annual review of sociology*, 27(1):415–444, 2001.
- [33] Adam Paszke, Sam Gross, Francisco Massa, Adam Lerer, James Bradbury, Gregory Chanan, Trevor Killeen, Zeming Lin, Natalia Gimelshein, Luca Antiga, Alban Desmaison, Andreas Kopf, Edward Yang, Zachary DeVito, Martin Raison, Alykhan Tejani, Sasank Chilamkurthy, Benoit Steiner, Lu Fang, Junjie Bai, and Soumith Chintala. Pytorch: An imperative style, high-performance deep learning library. In *Advances in Neural Information Processing Systems* 32, pages 8024–8035. Curran Associates, Inc., 2019.

- [34] Mason A Porter, Jukka-Pekka Onnela, Peter J Mucha, et al. Communities in networks. *Notices of the AMS*, 56(9):1082–1097, 2009.
- [35] Filippo Radicchi, Claudio Castellano, Federico Cecconi, Vittorio Loreto, and Domenico Parisi. Defining and identifying communities in networks. *Proceedings of the national academy of sciences*, 101(9):2658–2663, 2004.
- [36] José J. Ramasco, S. N. Dorogovtsev, and Romualdo Pastor-Satorras. Self-organization of collaboration networks. *Phys. Rev. E*, 70:036106, Sep 2004.
- [37] Felix Sattler, Klaus-Robert Müller, and Wojciech Samek. Clustered federated learning: Model-agnostic distributed multitask optimization under privacy constraints. *IEEE transactions on neural networks and learning systems*, 32(8):3710–3722, 2020.
- [38] Prithviraj Sen, Galileo Namata, Mustafa Bilgic, Lise Getoor, Brian Galligher, and Tina Eliassi-Rad. Collective classification in network data. *AI magazine*, 29(3):93–93, 2008.
- [39] Oleksandr Shchur, Maximilian Mumme, Aleksandar Bojchevski, and Stephan Günnemann. Pitfalls of graph neural network evaluation. *arXiv preprint arXiv:1811.05868*, 2018.
- [40] Petar Velickovic, Guillem Cucurull, Arantxa Casanova, Adriana Romero, Pietro Liò, and Yoshua Bengio. Graph attention networks. In *6th International Conference on Learning Representations, ICLR 2018, Vancouver, BC, Canada, April 30 - May 3, 2018, Conference Track Proceedings*, 2018.
- [41] Hongyi Wang, Mikhail Yurochkin, Yuekai Sun, Dimitris Papailiopoulos, and Yasaman Khazaeni. Federated learning with matched averaging. In *International Conference on Learning Representations*, 2020.
- [42] Chuhan Wu, Fangzhao Wu, Yang Cao, Yongfeng Huang, and Xing Xie. Fedgmn: Federated graph neural network for privacy-preserving recommendation. *KDD*, 2021.
- [43] Chuhan Wu, Fangzhao Wu, Lingjuan Lyu, Tao Qi, Yongfeng Huang, and Xing Xie. A federated graph neural network framework for privacy-preserving personalization. *Nature Communications*, 13(1):1–10, 2022.
- [44] Zonghan Wu, Shirui Pan, Fengwen Chen, Guodong Long, Chengqi Zhang, and Philip S. Yu. A comprehensive survey on graph neural networks. *IEEE Trans. Neural Networks Learn. Syst.*, 32(1):4–24, 2021.
- [45] Han Xie, Jing Ma, Li Xiong, and Carl Yang. Federated graph classification over non-iid graphs. In *Advances in Neural Information Processing Systems*, volume 34, pages 18839–18852. Curran Associates, Inc., 2021.
- [46] Ke Zhang, Carl Yang, Xiaoxiao Li, Lichao Sun, and Siu Ming Yiu. Subgraph federated learning with missing neighbor generation. In *Advances in Neural Information Processing Systems*, volume 34, pages 6671–6682. Curran Associates, Inc., 2021.
- [47] Michael Zhang, Karan Sapra, Sanja Fidler, Serena Yeung, and Jose M. Alvarez. Personalized federated learning with first order model optimization. In *International Conference on Learning Representations*, 2021.
- [48] Muhan Zhang and Yixin Chen. Link prediction based on graph neural networks. In *Advances in Neural Information Processing Systems 31: Annual Conference on Neural Information Processing Systems 2018, NeurIPS 2018, December 3-8, 2018, Montréal, Canada*, pages 5171–5181, 2018.
- [49] Jie Zhou, Ganqu Cui, Shengding Hu, Zhengyan Zhang, Cheng Yang, Zhiyuan Liu, Lifeng Wang, Changcheng Li, and Maosong Sun. Graph neural networks: A review of methods and applications. *AI Open*, 1:57–81, 2020.

# Appendix

**Organization** This appendix is organized as follows. In Section A, we first describe the algorithms of our FEDerated Personalized sUBgraph learning (FED-PUB) framework, on both server- and client-sides. Then, we provide the detailed experimental setups including datasets, models and hyperparameters in Section B, as well as the additional experimental results in Section C. After that, we finally discuss the limitations and potential societal impacts of our work in Section D.

## A Algorithms

In this section, we algorithmically describe where the proposed subgraph similarity estimation and adaptive weight masking are performed in our FED-PUB framework, which is shown in Algorithm 1 for the client and in Algorithm 2 for the server.

Algorithm 1 FED-PUB Client Algorithm	Algorithm 2 FED-PUB Server Algorithm
1: $R$ : number of rounds, $E$ : number of epochs, $K$ : number of clients, $\mathcal{D}_k$ : local data for client $k$ , $f_k$ : model function for client $k$ , $\theta_k$ : model parameters for client $k$ , $\mu_k$ : weight masking parameters for client $k$ , $\mathcal{S}(\cdot)$ : similarity matching function, $\tau$ : scaling factor for similarity matching. 2: <b>Function</b> RunClient( $\bar{\theta}_k$ ) 3: $\theta_k \leftarrow \bar{\theta}_k \otimes \mu_k$ 4: <b>for</b> each local epoch $e$ from 1 to $E$ <b>do</b> 5: $\theta_k \leftarrow \theta_k - \eta \nabla \mathcal{L}(\mathcal{D}_k; \theta_k, \mu_k)$ 6: <b>end for</b> 7: <b>return</b> $\theta_k$	1: <b>Function</b> RunServer() 2: initialize $\bar{\theta}^{(0)}$ 3: <b>for</b> each round $r = 1, 2, \dots, R$ <b>do</b> 4: <b>for</b> $f_k \forall k$ <b>in parallel do</b> 5: <b>if</b> $r = 1$ <b>then</b> 6: $\theta_k^{(r+1)} \leftarrow \text{RunClient}(\bar{\theta}^{(r)})$ 7: <b>else</b> 8: $\bar{\theta}_k^{(r)} \leftarrow \sum_{i=0}^K \frac{\exp(\tau \cdot \mathcal{S}(k,i))}{\sum_{j=0}^K \exp(\tau \cdot \mathcal{S}(k,j))} \theta_i$ 9: $\theta_k^{(r+1)} \leftarrow \text{RunClient}(\bar{\theta}_k^{(r)})$ 10: <b>end if</b> 11: <b>end for</b> 12: <b>end for</b>

## B Experimental Setups

In this section, we first provide the descriptions of six different benchmark datasets that we use, with their preprocessing setups and statistics in Subsection B.1. Then, we introduce the baselines and our proposed FED-PUB in detail in Subsection B.2. After that, we further describe the implementation details of the experiments on synthetic and real-world graphs in Subsection B.3.

### B.1 Datasets

We report the statistics of six different benchmark datasets (i.e., Cora, CiteSeer, Pubmed, and ogbn-arxiv for citation graphs; Computer and Photo for amazon product graphs) [38, 17, 30, 39] that we use in our experiments for both the overlapping and non-overlapping node scenarios, in Table 3. For dataset splits, we randomly select 20% nodes for training, 35% for validation, and 35% for testing, for all datasets except for the arxiv dataset. As the arxiv dataset has relatively larger numbers of nodes as shown in Table 3, we randomly select 5% nodes for training, the remaining half of the nodes for validation, and the other nodes for testing.

We then describe how to partition the original graph into multiple subgraphs, whose counts are the same as the number of clients. In general, we use the METIS graph partitioning algorithm [21] to divide the original graph into multiple subgraphs, which can control the number of disjoint subgraphs as parameters. Thus, in the non-overlapping node scenario, the disjoint subgraphs for each client are directly obtained by the output of the METIS algorithm (i.e., if we set the parameter value for METIS as 10, then we can obtain the 10 different disjoint subgraphs, each of which is given to each client). On the other hand, in the overlapping node scenario where nodes are duplicated across different subgraphs, we first divide the original graph into 2, 6, and 10 disjoint subgraphs for 10 clients, 30 clients, and 50 clients, respectively, with the METIS algorithm. After that, in the one disjoint subgraph, we randomly sample half of the nodes and their associated edges, and then use

Table 3: **Statistics of datasets**, where we report the number of nodes, edges and classes for both the original graph and its splitted subgraphs. Ori denotes the original graph, and Cli denotes the number of clients.

<i>Overlapping node scenario</i>												
	Cora				CiteSeer				Pubmed			
	Ori	10 Cli	30 Cli	50 Cli	Ori	10 Cli	30 Cli	50 Cli	Ori	10 Cli	30 Cli	50 Cli
# Classes		7				6				3		
# Nodes	2,485	621	207	124	2,120	530	177	106	19,717	4,929	1,643	986
# Edges	10,138	1,249	379	215	7,358	889	293	170	88,648	10,675	3,374	1,903
	ogbn-arxiv				Amazon-Computer				Amazon-Photo			
	Ori	10 Cli	30 Cli	50 Cli	Ori	10 Cli	30 Cli	50 Cli	Ori	10 Cli	30 Cli	50 Cli
# Classes		40				10				8		
# Nodes	169,343	42,336	14,112	8,467	13,381	3,345	1,115	669	7,487	1,872	624	374
# Edges	2,315,598	282,083	83,770	44,712	491,556	59,236	16,684	8,969	238,086	29,223	8,735	4,840
<i>Non-overlapping node scenario</i>												
	Cora				CiteSeer				Pubmed			
	Ori	5 Cli	10 Cli	20 Cli	Ori	5 Cli	10 Cli	20 Cli	Ori	5 Cli	10 Cli	20 Cli
# Classes		7				6				3		
# Nodes	2,485	497	249	124	2,120	424	212	106	19,717	3,943	1,972	986
# Edges	10,138	1,866	891	422	7,358	1,410	675	326	88,648	16,374	7,671	3,607
	ogbn-arxiv				Amazon-Computer				Amazon-Photo			
	Ori	5 Cli	10 Cli	20 Cli	Ori	5 Cli	10 Cli	20 Cli	Ori	5 Cli	10 Cli	20 Cli
# Classes		40				10				8		
# Nodes	169,343	33,869	16,934	8,467	13,381	2,676	1,338	669	7,487	1,497	749	374
# Edges	2,315,598	410,948	182,226	86,755	491,556	84,480	36,136	15,632	238,086	43,138	19,322	8,547

them as the subgraph for one particular client. This procedure is performed five times to generate five different yet overlapped subgraphs for five clients, per one split subgraph obtained from METIS.

## B.2 Baselines and Our Model

1. **FedAvg**: This method [31] is the FL baseline, where each client locally updates a model and then sends it to a server, while the server aggregates the locally updated models with respect to their number of training samples and then transmits the aggregated one back to the clients.
2. **FedProx**: This method [26] is the FL baseline, which regularizes the local model to not drift too much to the local data by minimizing the weight differences between local and global models.
3. **FedPer**: This method [2] is the personalized FL baseline, which shares only the base layers, while keeping the personalized classification layers in the local side.
4. **FedGNN (FedPerGNN)**: This method [42, 43] is the subgraph FL baseline, which expands the local subgraph by exactly augmenting the relevant nodes from the other clients. The relevant nodes are selected based on the similarity between the nodes in the local client and the other nodes in other clients. Note that the authors of FedGNN [42] simply extend it to FedPerGNN [43] while keeping its core algorithm: naive averaging of gradients from all clients for model aggregation.
5. **FedSage**: This method [46] is the subgraph FL baseline, which expands the local subgraph by estimating the nodes from the local graph generator that is trained with the information of nodes in the other clients. Specifically, to train the graph generator, it first transmits the local node representations to other clients, and then calculates the gradient of the distance between received node representations and local node representations, which are transmitted back to the local client.
6. **GCFL**: This method [45] is the graph FL baseline, which targets completely disjoint graphs (e.g., molecular graphs) as in image tasks. In particular, this method uses the bi-partitioning scheme, which divides a set of clients into two disjoint client groups based on their similarity of gradients. Then, the model weights are only shared between grouped clients having similar gradients, after partitioning. Note that this bi-partitioning scheme is similar to the scheme proposed in clustered-FL [37] for image classification, and we adopt this for our subgraph FL.
7. **Local**: This method is the non-FL baseline, which only locally trains the model for each client, and does not share weights between clients.
8. **FED-PUB**: This is our FEDERated Personalized sUBgraph learning (FED-PUB) framework, which not only estimates the similarity between client subgraphs with their models' functional embeddings for detecting subgraph community structures, but also adaptively masks received weights from the server for selecting only the subgraph-relevant parameters.

### B.3 Implementation Details

**Implementation Details on Sparse Masks** As described in Section 4.2, we propose to sparsify the local personalized mask  $\mu_k$  for each client  $k$ , for taking advantages of efficiencies in communication and prediction costs. In this paragraph, we additionally provide the detailed implementation specifications on sparse masks during the training and test phases of our FED-PUB. First, in training, we regularize the local mask  $\mu_k$  to be sparse by minimizing the  $L_1$  Norm of it along with its scaling parameter  $\lambda_2$  to the local loss  $\mathcal{L}$ , represented in equation 5. However, this regularization scheme might not be enough to exactly make a subset of local masks zero. Therefore, in the test phase, we use the threshold scheme, where elements (neurons) of  $\mu_k$  below a certain threshold (i.e.,  $\lambda_2$ ) are set to zero. By doing so, we can transmit only the partial parameters to the server, but also can predict with only the partial parameters, therefore, effectively reducing communication and prediction costs.

**Common Experimental Details** For all experiments, we stack two layers of Graph Convolutional Network (GCN) [23] and one linear classifier layer. Also, the number of hidden dimensions is set to 128, the learning rate is set to 0.001, and all clients participate in federated training for every round. Then, all models are optimized with Adam optimizer [22]. To obtain functional embeddings in our FED-PER framework, we randomly generate a community graph from a stochastic block model [16]. Specifically, we sample five different graphs each of which has 100 nodes, where the probability of edges within the single graph is 0.1, while the probability of edges between the different graphs is 0.0. The node features for the sampled community graph are randomly initialized from the normal distribution. Note that the randomly sampled graphs are initialized at the server-side and the server distributes such graphs to all clients, while the client calculates its model’s functional embedding and then transmits the obtained embedding to the server. Furthermore, for all experiments about our FED-PUB, we set the  $\lambda_1$  and  $\lambda_2$  for  $L_1$  and  $L_2$  losses for sparsity and proximal terms as 0.001. Notably, while we can tune such two scaling hyperparameters, we observe that those two values show satisfactory performances across all datasets without further specific tuning to each dataset.

**Experimental Details on Synthetic Graphs** We perform two experiments on synthetic graphs, which are shown in Figure 1 and Figure 3 of the main paper. In particular, in the experiment of Figure 1, there are three communities that have different label distributions (e.g., the nodes in the first community have label 0, whereas the nodes in the last community have label 2), and each community has 5/5/40 non-overlapped subgraphs. Also, there are 50 clients, and each client has one of 50 subgraphs. Each subgraph consists of 30 nodes, and the edges between two nodes are sampled from the probability of 0.5. Also, in the experiment of Figure 3, there are two communities that have different label distributions, and each community has 5/15 non-overlapped subgraphs. Also, there are 20 clients, and each client has one of 20 subgraphs. Each subgraph consists of 30 nodes, and the edges between two subgraphs within the same community are sampled from the probability of 0.7, whereas the edges between two subgraphs from different communities are sampled from the probability of 0.01. For all experiments, the number of local epochs is set to 3, and the number of total rounds is set to 100. In our FED-PER including its variants of using parameter and gradient, the scaling hyperparameter for calculating the similarity in equation 4 (i.e.,  $\tau$ ) is set to 10.

**Experimental Details on Real-World Benchmark Graphs** For small datasets, namely Cora, CiteSeer and PubMed, we set the number of local training epoch as 1, and the number of total rounds as 100. Also, for larger datasets, such as Computer, Photo and arxiv, we set the number of total rounds as 200, while the number of local epochs is set to 2 for Photo and arxiv, and set to 3 for Computer. In the overlapping node scenario, we set the similarity scaling hyperparameter (i.e.,  $\tau$ ) as 5 for all our models. Meanwhile, we set the similarity scaling hyperparameter (i.e.,  $\tau$ ) as 3 in the non-overlapping node scenario for all our models. We generally observe that, the larger  $\tau$  value works better for the overlapping node scenario, in which different subgraphs are easily grouped together, compared to the non-overlapping node scenario. Finally, we report the test performance of all models at the best validation epoch, and the performance is measured by the node classification accuracy.

**Computing Resources** For all experiments, we use PyTorch [33] and PyTorch Geometric [8] as deep learning libraries. We use two types of GPUs: GeForce RTX 2080 Ti and TITAN XP for training each model. The runtime of our framework depends on the number of clients, and also workers for processing clients’ jobs, as well as the number of local epochs and rounds. In general, we use 10 or 20 workers (i.e., simultaneously training 10/20 local models for 10/20 clients), and the single run of our algorithm for 50 clients with 1 local epoch and 100 total rounds takes less than 2 hours.

$\lambda_1$	$\lambda_2$	Accuracy [%]	Sparsity [%]	$\lambda_1$	$\lambda_2$	Accuracy [%]	Sparsity [%]
3e-1	1e-3	79.62 $\pm$ 0.23	28.93 $\pm$ 0.52	7e-1	1e-3	78.68 $\pm$ 0.59	56.94 $\pm$ 0.29
5e-1	1e-3	79.42 $\pm$ 0.37	42.38 $\pm$ 0.35	7e-1	1e-2	78.56 $\pm$ 0.05	56.61 $\pm$ 0.32
7e-1	1e-3	78.68 $\pm$ 0.59	56.94 $\pm$ 0.29	7e-1	1e-1	79.46 $\pm$ 0.41	57.41 $\pm$ 1.33
9e-1	1e-3	77.36 $\pm$ 0.99	74.87 $\pm$ 0.34	7e-1	1e-0	79.31 $\pm$ 0.45	57.28 $\pm$ 0.16

Figure 11: Analysis on hyperparameters  $\lambda_1$  and  $\lambda_2$ , with corresponding model sparsity and performance.

## C Additional Experimental Results

### C.1 Results of $\lambda_1$ and $\lambda_2$ Experiments

In Figure 11, we further explore the effects of hyperparameters  $\lambda_1$  and  $\lambda_2$  on the Cora dataset with the overlapping node scenario, where the number of local epochs is set as 2 and the number of clients is set as 10. In particular,  $\lambda_1$  value can control the degree of the model sparsity, thus, to see its efficacy, we fix  $\lambda_2$  value while varying  $\lambda_1$ , and then measure both the model sparsity and performance. As shown in Figure 11 left, higher  $\lambda_1$  values significantly increase the model sparsity, meanwhile, the model performance is slightly decreased. The results indicate that we should consider the trade-off between the sparsity and the model performance, when choosing the  $\lambda_1$  value. On the other hand,  $\lambda_2$  value is designed to prevent the excessive knowledge drift to the local subgraph distributions, and, to verify its effectiveness, we fix  $\lambda_1$  value while varying  $\lambda_2$ . As shown in Figure 11 right, too small lambda values lead to the performance degeneration, thus choosing the sufficiently large  $\lambda_2$  values (e.g., 1e-1) would lead to the performance improvement. Also, we further observe that the sparsity does not depend on  $\lambda_2$  value, thus the effects of  $\lambda_1$  and  $\lambda_2$  are orthogonal and complementary.

## D Limitations and Potential Societal Impacts

In this section, we discuss the limitations and potential societal impacts of our work.

**Limitations** While our personalized subgraph FL framework, namely FED-PUB, is generally applicable regardless of the types of subgraphs (e.g., unipartite graphs or bipartite graphs), our experiments are mainly done with unipartite graphs which are the most popular graph representation learning settings. However, the behaviors of our FED-PUB on the other types of graphs, such as bipartite graphs, would be interesting to further see, which is but not been explored so far, and we leave this as future work.

**Potential Societal Impacts** The FL scheme is important for preserving users’ privacy, and, while this scheme is actively studied in the image and language domains, it gets little attention for graphs. In particular, the subgraph FL, which we mainly target, has unique challenges on missing nodes, edges, and their community structures, and we believe which are sufficiently tackled in our work.

Then, the potential positive impact of our work on society is that, our method affects various domains that use graphs, such as social networks, recommendation networks, and patient networks, to name a few. Note that we would like to emphasize the importance of our subgraph FL scheme, especially in social and recommendation networks. In the current real-world applications, all the user’s interactions with other users for social networks and with other products for recommendation networks may be stored in the server. However, this may not preserve the user’s privacy, but also has potential risks of a leak of user data from the server, such that storing the user’s data in the server is not recommended, for example, from the data protection regularizations such as GDPR<sup>5</sup>. Then, by applying our subgraph FL framework to this domain, we expect such problems could be resolved by not storing user’s interaction data to the server, but only sharing the locally trained models with clients.

However, the transmitted model parameters from the client to the server may hold the privacy-sensitive information, and, while this is not the main focus of this work (i.e., we assume that model parameters are transmittable without compromising privacy as in many FL works [31, 26, 2]), the research community may need to put further attention about whether the model parameters is safe, and how to make them safe if the model parameters contain privacy-sensitive information.

<sup>5</sup><https://gdpr-info.eu/>